Multichannel Reaction of C_2Cl_3 + O_2 Studied by Time-Resolved Fourier Transform Infrared Emission Spectroscopy[†]

Tiancheng Xiang,[‡] Kunhui Liu,[‡] Shaolei Zhao,[‡] Hongmei Su,*,[‡] Fanao Kong,[‡] and Baoshan Wang[§]

State Key Laboratory of Molecular Reaction Dynamics and Beijing National Laboratory for Molecular Sciences (BNLMS), Institute of Chemistry, Chinese Academy of Sciences, Beijing 100080, People's Republic of China, and College of Chemistry and Molecular Sciences, Wuhan University, Wuhan 430072, People's Republic of China

The multichannel reaction of the C_2Cl_3 radical with O_2 has been studied thoroughly by step-scan time-resolved Fourier transform infrared emission spectroscopy. Vibrationally excited products of Cl_2CO, CO, and CO_2 are observed and three major reaction channels forming respectively $ClCO$ + Cl_2CO, CO + CCl_3O, and CO_2 + CCl_3 are identified. The vibrational state distribution of the product CO is derived from the spectral fitting, and the nascent average vibrational energy of CO is determined to be 59.9 kJ/mol. A surprisal analysis is applied to evaluate the vibrational energy disposal, which reveals that the experimentally measured CO vibrational energy is much more than that predicted by statistical model. Combining previous *ab initio* calculation results, the nonstatistical dynamics and mechanism are characterized to be barrierless addition–elimination via short-lived reaction intermediates including the peroxy intermediate C_2Cl_3OO* and a crucial three-member-ring COO intermediate.

1. Introduction

By reacting with C2 unsaturated hydrocarbons, vinyl radicals are believed to play critical roles in the formation of soot, PAH (polycyclic aromatic hydrocarbon), and coke in the combustion processes. On the other hand, the competing fast oxidation reaction of vinyl by O_2 molecules scavenges vinyl radicals and thus suppresses the formation of soot, PAH, and coke. A limited number of studies have been done on the reaction of vinyl with O_2 both experimentally and theoretically.[1] The major reaction channel of vinyl with O_2 is to form H_2CO and HCO through a three-member-ring intermediate:

$$C_2H_3 + O_2 \rightarrow HCO + H_2CO$$
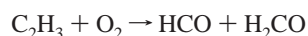
Wang et al.[2] also reported an observation of the channel to produce CO_2 and CH_3:

$$C_2H_3 + O_2 \rightarrow CO_2 + CH_3$$

Analogously, the chlorinated vinyl radical, C_2Cl_3, should also be taken into consideration as a critical reactive intermediate in the combustion of chlorinated hydrocarbons such as hazardous chemical and plastic wastes that frequently contain CHCs and thus leading to atmospheric pollution.[3] Despite its importance, studies on the reaction of C_2Cl_3 are rare. Experimentally, only the rate constant of this reaction has been measured by Russell et al.[3] using photoionization mass spectrometry over the temperature range 298–648 K. They reported the Arrhenius expression to be $2.0(\pm0.4) \times 10^{-12} \exp\{830(\pm230)/RT\}$, in units of cm^3 molecule^{-1} s^{-1} and cal mol^{-1} for the Arrhenius

activation energy, and the room-temperature reaction rate constant to be 8.2×10^{-12} cm^3 molecule^{-1} s^{-1}. Their experiment only indicated the product formation of Cl_2CO (phosgene) without solid evidence. Theoretically, we have recently reported the *ab initio* calculation results on the energetics of the following exothermic reaction channels.[4]

		ΔH (kJ·mol^{-1}) (calcd from heat of formation)
$C_2Cl_3 + O_2$	$\rightarrow ClCO + Cl_2CO$	−431.9
	$\rightarrow O(^3P) + C_2Cl_3O$	−89[4]
	$\rightarrow CO_2 + CCl_3$	−511.8
	$\rightarrow CO + CCl_3O$	−338.6
	$\rightarrow Cl + (ClCO)_2$	−404.5
	$\rightarrow Cl + CCl_2C(O)O$	−318[4]
	$\rightarrow CCl_2 + ClCO_2$	−186[4]
	$\rightarrow ClO + CCl_2CO$	−183.7

The calculation shows that all the above channels are energetically accessible. However, detailed experimental measurements of the reaction products and identification of the reaction channels have not been done previously. In this paper, we report our experimental investigation on the reaction products and channels by means of step-scan time-resolved Fourier transform infrared emission spectroscopy (TR-FTIR). TR-FTIR is an effective technique probing multiple IR-active reaction products in real time due to its multiplex advantage and nanosecond time resolution. By observing the vibrationally excited products from the time-resolved IR emission spectra, several major reaction channels are identified for this multi-channel free radical reaction. Moreover, the product vibrational energy disposal is derived from the spectral fitting and compared with that predicted by surprisal analysis. All of these experimental findings are discussed along with the *ab initio* calculation

results. New insights are gained concerning the products, channels, energy disposal, and mechanism for the C_2Cl_3 + O_2 reaction.

2. Experimental Section

The reaction products are monitored by step-scan, time-resolved Fourier transform emission spectroscopy.[5] This is an effective technique to acquire broad-band, time-resolved spectra of multiple products simultaneously.

Step-scan FTIR spectrometers are commercially available but require significant modification for coupling with a pulsed laser to study photolysis initiated free radical reactions. This newly upgraded machine comprises a Nicolet Nexus 870 step-scan FTIR spectrometer, Lambda Physik (LPX305i) Excimer laser, and a pulse generator (Standford Research DG535) to initiate the laser pulse and achieve synchronization of the laser with data collection, two digitizers (internal 100 kHz 16-bit digitizer and external 100 MHz 14-bit GAGE 8012A digitizer), which offer fast time resolution and a wide dynamic range as needed, and a personal computer to control the whole experiment. The detector used in this experiment is either a liquid nitrogen cooled InSb detector or MCT-A detector.

The reaction is initiated in a stainless steel flow reaction chamber. A pair of parallel multilayer coated mirrors (reflectivity $R > 0.95$ at 248 nm) reflect the UV laser beam multiple times to increase the photolysis zone. C_2Cl_3 radicals are generated by 248 nm photodissociation (100 mJ cm^{-2} pulse^{-1}, 10 Hz repetition rate) of C_2Cl_4. Samples of C_2Cl_4 ($\geq$99%) and O_2 ($\geq$99.5%) enter the flow chamber 1 cm above the photolysis beam via needle valves. The chamber is pumped by an 8 L s^{-1} mechanical pump, and the stagnation pressure of the chamber is measured by a MKS capacitance manometer. The constant pressure of the sample is maintained by adjusting the pumping speed and the needle valves. Typically, C_2Cl_4 (100 mTorr) and O_2 (650 mTorr) are used to keep pseudo-first-order reaction conditions and minimizing secondary reactions of the C_2Cl_3 radicals. Transient infrared emission is collected by a pair of gold-coated White-Cell spherical mirrors and collimated by a CaF$_2$ lens to a step-scan Fourier spectrometer Nicolet Nexus 870. The spectrometer and the collimating tube are both flushed with N$_2$ to eliminate the environmental CO_2 absorption to IR emissions.

With the 8 L s^{-1} pumping speed, the e-fold pump down time in the 20-L-volume reaction cell is equal to several seconds. However, the photolysis volume in the cylinder, 250 mL, is evacuated on a time scale of tens of milliseconds, which is likely to be a more accurate measure of the residence time of the reactive gas mixture. Thus, it is expected that the flow rate is fast enough to replenish the sample at each laser pulse running normally at a repetition rate of 10 Hz. A buildup of certain reaction products could complicate the chemistry. To test whether this was affecting the present results, the experiment was run at 2 Hz in addition to the normal 10 Hz; the slower repetition rate would significantly decreases any buildup of reaction products between laser pulses. Decreasing the repetition rate caused no discernible effect in the observed time-dependent IR spectra for the gas flows used herein.

The response function of the instrument was measured using a blackbody source (Gemini R Model 976, Isothermal Technology LTD) maintained at 773 K. The instrumental response function represents the spectral response of the detector and the reflectivity or transmittance of the optics. Generally, the measured IR emission intensity should be corrected by the instrumental response function. However, for the specific

spectral range (the CO IR emission band: from 1900 to 2200 cm^{-1}) that we are to determine the vibrational population distribution by fitting the IR emission intensities, the instrumental responsivity keeps constant with wavelength. The variation of the responsivity from 1900 to 2200 cm^{-1} is within 3%, even less than the fluctuation of the signal itself (roughly 7%). Considering the above-mentioned fact, we did not try to correct the IR emission intensities by instrumental response function within this specific spectral range.

3. Results and Discussion

3.1. Photolytic Source of C_2Cl_3 Radicals. In this experiment, C_2Cl_3 radicals were generated by 248 nm KrF laser photolysis of C_2Cl_4. To avoid the existence of multiphoton processes, the 248 nm laser beam was diverged when reaching the sample by focusing outside of the reaction vessel. The laser power dependence of the product signal is linear, ruling out two photon dissociation processes.

Even radiated at a low power density, the one-photon photodissociation process of C_2Cl_4 molecules are expected to follow two pathways:

$$C_2Cl_4 \rightarrow C_2Cl_3 + Cl$$
$$\rightarrow C_2Cl_2 + Cl_2$$
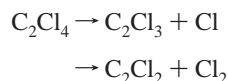
Russell et al.[3] observed the formation of both the photoproducts C_2Cl_3 and C_2Cl_2, indicating that the two pathways are of equal importance.

Fortunately, all the possibly interfering photofragments, i.e., Cl atoms and C_2Cl_2 molecules are benign and not likely to react with O_2. The possible following reactions of the Cl atoms with O_2 are either endothermic or slightly exothermic and thus can be neglected.

$$Cl + O_2 \rightarrow ClO + O \quad \Delta H = 228.2 \text{ kJ/mol}$$
$$\rightarrow ClOO \quad \Delta H = -21.7 \text{ kJ/mol}$$
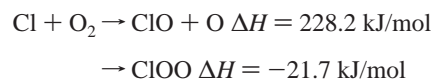
The other photofragments, the chlorinated acetylene C_2Cl_2 and Cl_2 are stable molecules. They are not expected to react with O_2 molecules as fast as the radical fragment C_2Cl_3 (the reaction rate constant of C_2Cl_3 radical with O_2 was reported to be 8.2×10^{-12} cm^3 molecule^{-1} s^{-1} at room temperature[3]). Therefore, all the coexisted photofragments Cl atoms, Cl_2 molecules, and chlorinated acetylenes C_2Cl_2 are not likely to compete with the highly reactive C_2Cl_3 radicals in their reaction with O_2 molecules. The photodissociation of C_2Cl_4 molecules provide a good source of C_2Cl_3 radicals.

3.2. Identification of the Elementary Reaction Products. TR-FTIR emission spectroscopy can detect multiple vibrationally excited species simultaneously. In this experiment, vibrationally excited species may arise from the hot photolysis fragments and the products of the consecutive radical reactions. We observed no IR emission signals from the pure photodissociation of C_2Cl_4. This provides a background free detection of the reaction of C_2Cl_3 with O_2.

When the mixture of 100 mTorr of C_2Cl_4 and 650 mTorr of O_2 was irradiated by 248 nm laser, strong IR emission signals were detected. Figure 1 shows a series of TR-FTIR emission spectra at typical delay times from 5 to 120 μs after the initiation of the reaction by photolysis laser with a 0.5 cm^{-1} spectral resolution. Three emission bands were observed, as shown in the spectra collected at the early reaction time of 5 and 10 μs. One weak emission band is peaked at 1850 cm^{-1}, and the other
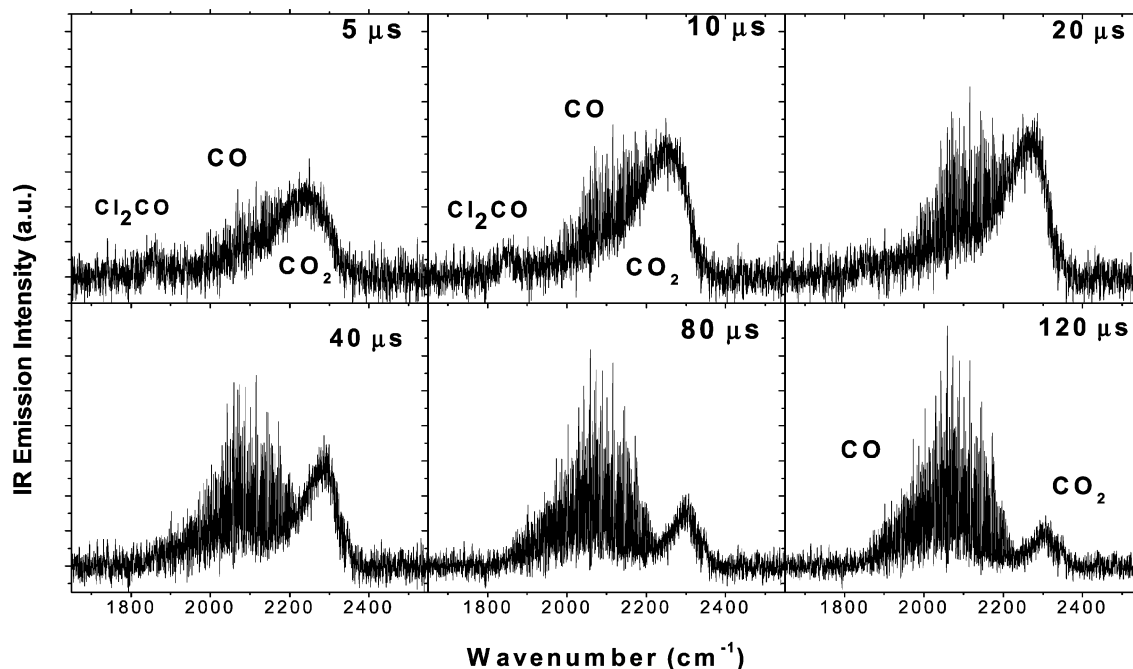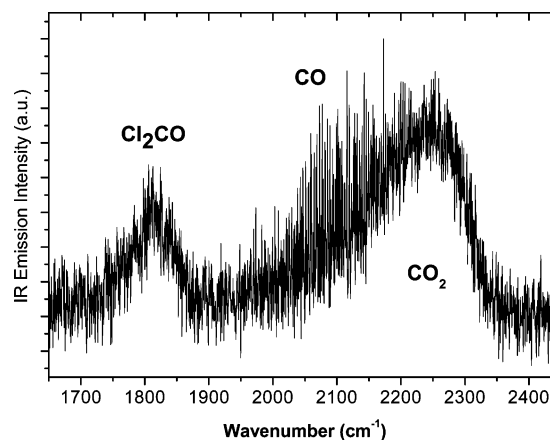
Figure 1. Product TR-FTIR emission spectra from the reaction of $C_2Cl_3 + O_2$ taken at typical reaction times from 5 to 120 μs after initiation of the reaction by 248 nm laser photolysis. The spectra were collected using the detector of InSb with the spectral resolution of 0.5 cm^{-1}.

two strong emission bands spread over the spectral region from 1940 to 2370 cm^{-1}.

The strong emission band spanning from 1940 to 2370 cm^{-1} actually arises from two species. The fully rotationally resolve-demission lines from 1940 to 2200 cm^{-1} are due to $\Delta v = -1$ transitions of vibrationally excited $CO(v'=1-10)$. The CO emission grows monotonically with time and reaches an asymptote at 80 μs. The intensity of CO emission band hardly decays and sustains until the millisecond time scale. The CO rovibrational lines are superimposed on top of a broad partially resolved emission band spanning from 2100 to 2370 cm^{-1}, which is due to $(\nu_1, \nu_2, \nu_3) \rightarrow (\nu_1, \nu_2, \nu_3 - 1)$ transitions of vibrationally excited CO_2.[6] Three modes of the CO_2 vibration might all be excited. Unlike the diatomic vibrationally excited molecule CO, the high density of the $(\nu_1, \nu_2, \nu_3) \rightarrow (\nu_1, \nu_2, \nu_3 - 1)$ transitions of CO_2 makes its rotational structure irresolvable at 0.5 cm^{-1} spectral resolution (the best resolution we can attain with this instrument).

Both products of CO and CO_2 are formed with significant internal excitation, leading to broad, red-shifted IR emission spectra. At early reaction times such as 5 and 10 μs the emission band of CO_2 spreads to the red and overlaps with the emission band of CO, indicating that CO_2 molecules are highly vibrationally excited. With increasing time, the CO_2 band blue shifts and cascades toward the band origin as the more energetic vibrational states are depopulated by collisional energy transfer until at 80 μs it is completely separated from the CO band. Eventually at 120 μs the CO_2 emission band relaxes to coincide in frequency with the CO_2 (001 $\rightarrow$ 000) band origin at 2349 cm^{-1}.

The weak emission band peaked at 1850 cm^{-1} shown in Figure 1 only reveals part of this band because the detector InSb cuts off at this position. Also, the intensity of this emission band is in fact underestimated. To obtain the full spectra of this species and measure its real intensity, we collected the spectra using the detector MCT-A with the detection sensitivity covering a spectral range of 720−5000 cm^{-1}, and the typical spectrum is shown in Figure 2. Although the sensitivity of MCT-A is only one-fifth as much as that of InSb, we were still

Figure 2. Product TR-FTIR emission spectra from the reaction of $C_2Cl_3 + O_2$ taken at 5 μs of the reaction time with the spectral resolution of 0.5 cm^{-1}. The spectra were collected using the lower sensitivity, but higher spectral range (720−5000 cm^{-1}) MCT-A detector.

able to collect high-resolution spectra by signal averaging multiple times and get a satisfactory S/N ratio. Indeed, there is really a more intense and broader emission band peaked at 1812 cm^{-1} observed with the detector MCT-A. Just like for the CO_2 band, the vibration-rotational structure of this band is irresolvable with the best resolution (0.5 cm^{-1}) attainable, indicating that it also arises from polyatomic molecules.

Simply judging from its spectral position (spanning from 1730 to 1870 cm^{-1}), this band should either arise from the C−O stretching (ν_1) mode of ClCO (vibrational fundamental frequency at 1884.6 cm^{-1})[7] or Cl_2CO (vibrational fundamental frequency at 1827 cm^{-1}). First, ClCO is highly unstable because C−Cl bond fission requires only 32.8 kJ/mol of energy.[8] The ClCO radicals generated from the reaction of $C_2Cl_3 + O_2$ are highly energized because the reaction channel forming ClCO + Cl_2CO releases 431.9 kJ/mol of energy. Therefore, the ClCO radicals are expected to decompose instantaneously once formed and thus will not be detected in the IR emission spectra. Wu[8] et al. did not observe the IR emission of ClCO near 1880 cm^{-1} in the photodissociation experiment of oxalyl chloride at
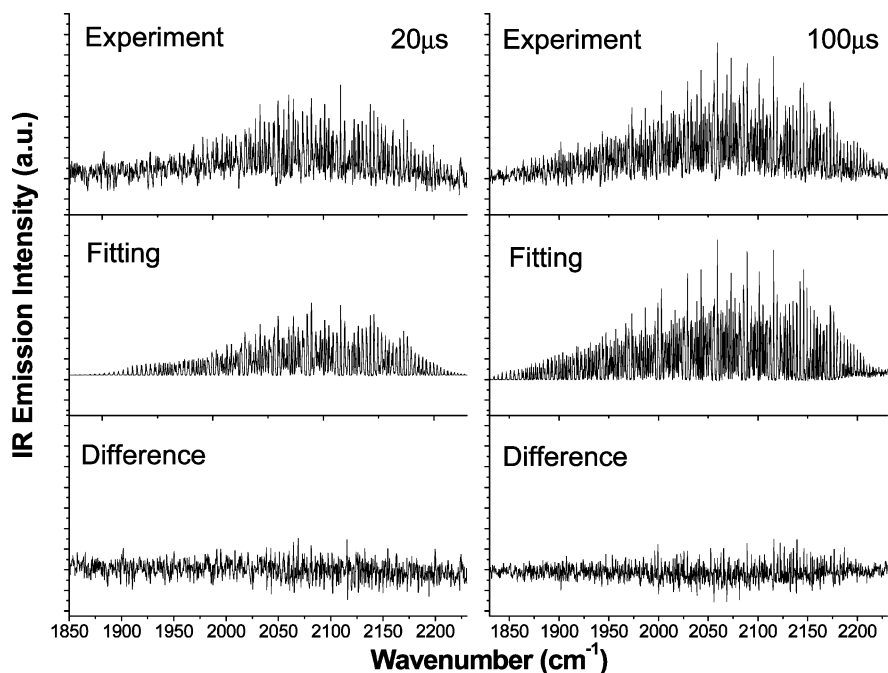
Figure 3. Representative spectral fitting results for the IR emission bands of the products CO at two reaction times of 20 and 100 μs. The difference between the experimental spectrum and the corresponding fitted spectrum is also shown at the bottom.

248 nm, which should generate ClCO fragments. They also ascribed this fact to the fast decomposition of the hot ClCO with an average internal energy of 63.8 kJ/mol. On the other hand, this emission band is most likely arising from the vibrationally excited product Cl_2CO because Cl_2CO molecules are highly stable. The bond fission of Cl_2CO requires 312.9 kJ/mol of energy and surmounting a barrier of 341.7 kJ/mol.[9] The vibrational relaxation of Cl_2CO molecules is extremely fast, as manifested by the rapid disappearance of its emission band at 20 μs, shown in Figure 1.

3.3. Vibrational State Distribution of the Product CO. Due to the advantage of broad band and the nature of IR emission, TR-FTIR emission spectra can provide the information of an almost complete vibrational state distribution. The vibrational state distribution is usually acquired by spectral fitting to experimental IR spectra using nonlinear least-squares fitting procedures.[10] For the three observed product species, only the diatomic molecule CO shows a rotationally resolved IR spectrum, whereas the spectra of the other two polyatomic species CO_2 and Cl_2CO are simply featureless, only showing an unresolved contour resulting from superimposition of numerous rovibrational transitions. With multiple vibrational modes present, the fitting to polyatomic molecules is normally more complicated. On the other hand, the fitting to the current spectra of featureless polyatomic species is presumably not plausible to yield unique fitting results and meaningful vibrational population. Therefore, only the rotationally resolved IR emission spectra of the diatomic products CO are analyzed by spectral fitting.

For spectra collected at early reaction times when CO_2 overlaps with CO, it is first required to remove the continuous band of CO_2 from the sharp features of CO and extract a spectrum that contains contribution only from CO. The extraction of CO_2 spectrum is done by judiciously choosing wavenumbers in the range 1940–2370 cm⁻¹ that lie between the sharp CO lines.[6] Then the pure CO spectrum is obtained by subtracting the CO_2 continuous spectrum from the overlapped spectrum.

The emission intensity for the diatomic product CO is fit using a nonlinear least-squares fitting program that has been described in detail previously.[11] Satisfactory fitting results are obtained, as demonstrated in Figure 3 by the representative fitting to two particular time slices (the left column shows the fitting results to the CO spectrum extracted from the 20 μs overlapped CO/CO_2 spectrum, the right column shows the fitting results to the already isolated CO spectrum at 100 μs). The spectral fitting yields the vibrational populations and rotational temperature. The rotational temperature of 300 K always generates the best fitting results, indicating that the rotational excitation has been thermalized. This is reasonable because these spectra are acquired as early as 5 μs after photolysis, corresponding to roughly 50 collisions (with total pressure of 750 millitorr), sufficient to equilibrate rotational distribution.

The populations at each vibrational level are derived from spectral fitting. For example, from the fittings displayed in Figure 3, the populations are 0.33/0.27/0.16/0.09/0.07/0.04/0.04 for the vibrational levels of $v' = 1-7$ at 20 μs. These populations can be well described by Boltzmann vibrational distribution as manifested in Figure 4. The average vibrational energy can be calculated from the normalized vibrational population N_v using the equation of $\langle E_{vib} \rangle = \sum_{V=1}^{V_{max}} N_V E_V$. The average vibrational energies of the product CO at 20 μs is thus calculated to be 63.5 kJ/mol.

Likewise, the average vibrational energy for CO at various reaction times are calculated and listed in Table 1. The average vibrational energy measured at 5 μs, 59.9 kJ/mol, is presumably very close to the nascent value. Only about 50 collisions occur in 5 μs, which does not alter much the vibrational distribution from the nascent one because the vibrational relaxation of CO is highly inefficient.[12,13] The colliding bath molecules O_2 and C_2Cl_4 in the system do not have any vibrational modes in resonance with the CO stretching (2140 cm⁻¹).

Using the reported reaction rate constant of 8.2×10^{-12} cm³ molecule⁻¹ s⁻¹,[3] it is estimated that the $C_2Cl_3 + O_2$ reaction should be complete (when the 99% of reactants are consumed) within 17 μs under the current pressure (100 mTorr of C_2Cl_4
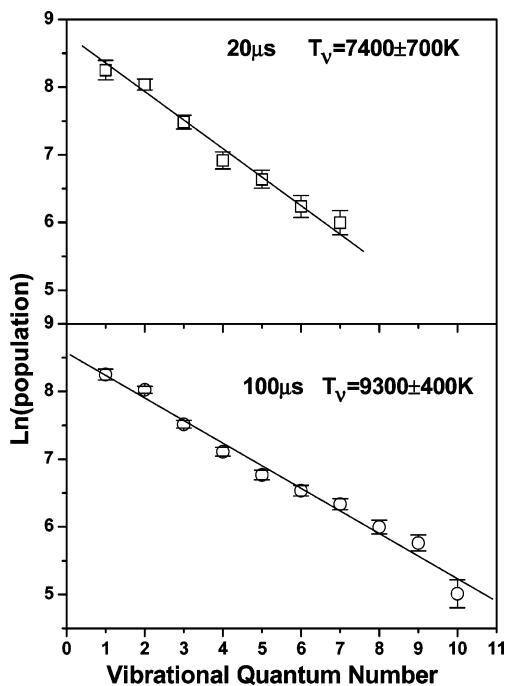
Figure 4. Representative Boltzmann plots of the vibrational distribution of CO from the $C_2Cl_3 + O_2$ reaction at two reaction times of 20 and 100 μs. The straight lines are the best fit of the data to a Boltzmann distribution with a temperature of 7400 ± 700 or 9300 ± 400 K, respectively.

TABLE 1: Average Vibrational Energy of CO at Various Reaction Times

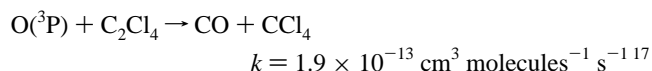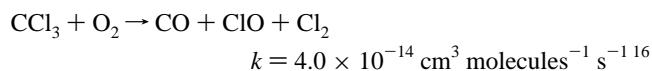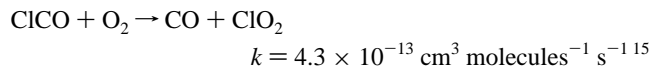| reacn time (μs)	5	10	20	30	40	50	60	80	100	120	160
E_V (kJ/mol)	59.9	61.7	63.5	69.5	70.5	73.4	76.6	78.5	78.2	78.0	77.8

and 650 mTorr of O_2). As shown in Figure 1, the formation rates of the Cl_2CO and CO_2 agree with the estimated reaction time, indicating that these two products are ascribed to the primary reaction of $C_2Cl_3 + O_2$. In contrast, the time evolution of another product CO, behaves differently. Both of the emission intensity and vibrational excitation of CO keeps increasing with time up to 120 μs. Most likely, secondary reactions play significant roles in the late formation of CO. To eliminate these secondary reactions, we have performed several reference experiments by decreasing both the pressure of precursor C_2Cl_4 (down to 50 mTorr) and O_2 molecules (down to 250 mTorr). No discernible difference of the IR emission spectra can be
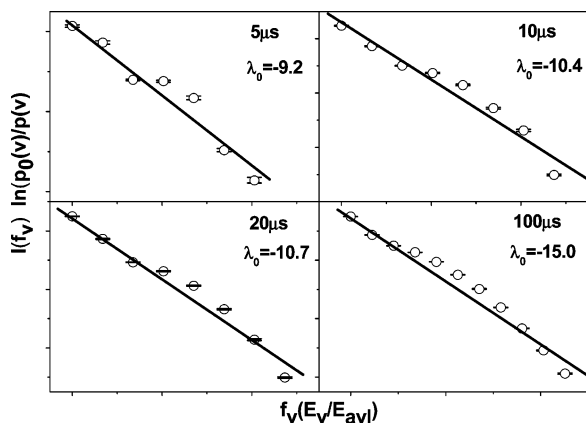
Figure 5. Representative surprisal plots for the fraction of the available energy in CO vibration at four reaction times of 5, 10, 20, and 100 μs. The corresponding surprisal parameters are derived to be −9.2, −10.4, −10.7, and −15.0, respectively.

observed for the low-pressure conditions, indicating that the secondary reactions cannot be avoided efficiently in the flow cell. On the other hand, the species partial pressures are necessarily maintained relatively high to ensure adequate signal-to-noise ratios in the IR emission detection experiment because of its low detection sensitivity relative to other methods. Consequently, secondary chemistry usually plays a role in the production of IR-active species, in this case, accounting for the formation of CO at late reaction times.[14]

Secondary radical−radical reactions are negligible due to their low concentration. The most probable secondary reactions forming CO are those of the primary radical products such as ClCO, CCl_3, and O (^{3}P) with the most abundant O_2 or C_2Cl_4 molecules: All of these possible secondary reactions are at least

$$ClCO + O_2 \rightarrow CO + ClO_2$$
$$k = 4.3 \times 10^{-13} \text{ cm}^3 \text{ molecules}^{-1} \text{ s}^{-1}\,[15]$$

$$CCl_3 + O_2 \rightarrow CO + ClO + Cl_2$$
$$k = 4.0 \times 10^{-14} \text{ cm}^3 \text{ molecules}^{-1} \text{ s}^{-1}\,[16]$$

$$O(^3P) + C_2Cl_4 \rightarrow CO + CCl_4$$
$$k = 1.9 \times 10^{-13} \text{ cm}^3 \text{ molecules}^{-1} \text{ s}^{-1}\,[17]$$

1 order of magnitude slower than the primary reaction of $C_2Cl_3 + O_2$. They are not likely to contribute to the formation of CO at early reaction times. Instead, the CO products observed at early reaction times should mainly arise from the primary reaction of the $C_2Cl_3 + O_2$. It is noticeable that CO is observed simultaneously with the other two primary reaction products of CO_2 and Cl_2CO as early as 5 μs, as shown in Figure 1.

3.4. Product Channels and Vibrational Energy Disposal. Vibrationally excited products of Cl_2CO, CO, and CO_2 are observed from the TR-FTIR emission spectra. The following reaction channels are therefore identified:

$$C_2Cl_3 + O_2 \rightarrow ClCO + Cl_2CO \qquad \Delta H = -431.9 \text{ kJ/mol} \quad (1)$$

$$\rightarrow CO + CCl_3O \qquad \Delta H = -338.6 \text{ kJ/mol} \quad (2)$$

$$\rightarrow CO_2 + CCl_3 \qquad \Delta H = -511.8 \text{ kJ/mol} \quad (3)$$

All these channels are highly exothermic, leading to vibrationally excited products. Channels 1 and 3 account for the production of Cl_2CO and CO_2, respectively. Channels 1 and 2 both contribute to the production of CO. In channel 2 CO is formed directly accompanied by the partner CCl_3O, the chlorinated methoxy radical. In channel 1, the highly unstable ClCO is expected to dissociate sequentially to CO readily as discussed in section 3.2.

A surprisal analysis is used to evaluate the vibrational energy disposal of the product CO.[18,19] As an example, Figure 5 shows the surprisal plots for the CO produced at several typical reaction times. The plots are basically linear. The statistical information-theoretic prior predicts an average vibrational energy of 25.5 kJ/mol for CO. The experimentally measured vibrational energy of 59.9 kJ/mol is much larger than the value predicted by the statistical model. Also, the surprisal parameters are negative, which means that the energy release into vibration is more than that of the prior distribution. Both indicate that the reaction is more likely to proceed through a direct reaction mechanism or short-lived reaction intermediates and hence the energy deposited into C−O bond initially in the reaction intermediate does not redistribute promptly before quick dissociation and forming final products. This is the usual case for exoergic reactions.[20]
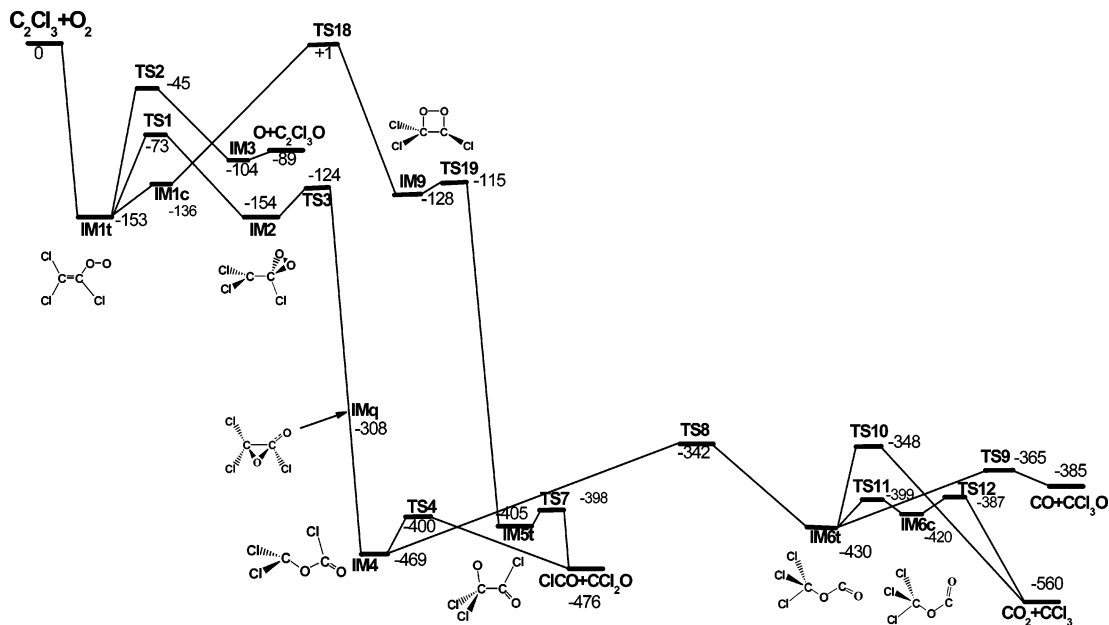
Figure 6. Energy diagram of the $C_2Cl_3 + O_2$ reaction paths.[4] The indicated energies (in kJ/mol) are obtained at the G3MP2//B3LYP/6-311G(d,p) level of theory. All the energies given are relative to the reactants, and structures of crucial reaction intermediates are shown too.

3.5. Comparison with the Computational Results. As a serial work prior to this one, we have performed a comprehensive *ab initio* calculation on the various paths of this reaction and detailed calculation results have been reported.[4] The energetics of the reactants, intermediates, transition states, and products along the reaction paths were calculated at the second-order Møller–Plesset Gaussain-3 level of theory (G3MP2) using the B3LYP/6-311G(d,p) optimized geometries. Figure 6 shows a concise energy diagram. Here, we only focus on comparing calculation results with experimental results in two aspects.

(1) Reaction Channels and Mechanism. The computational study reveals that the reaction proceeds through an addition–elimination mechanism by first forming a peroxy intermediate IM1t C_2Cl_3OO*. Starting from C_2Cl_3OO*, there are mainly two reaction paths. The energetically most favorable route is the isomerization of IM1t C_2Cl_3OO* into a three-member-ring intermediate IM2 and its subsequent isomerization to a highly energized intermediate IM4 with the C–O–C–O chain structure, which dissociates, forming eventually several final products including $ClCO + Cl_2CO$, $CO + CCl_3O$, $CO_2 + CCl_3$, etc. These channels are all highly exothermic. The second route involves a direct OO bond fission of C_2Cl_3OO* leading to the $O + C_2Cl_3O$ channel. The rate constants of these two reaction routes calculated on the basis of the variational transition state theory show that the reaction channels forming $ClCO + Cl_2$-CO, $CO + CCl_3O$, and $CO_2 + CCl_3$ are predominant over the channel forming $O + C_2Cl_3O$, although the latter one involves much less molecular rearrangements. These computational results explain quite well our experimental observation of the intense IR emission bands due to the vibrationally excited products of Cl_2CO, CO, and CO_2 and validate further the identification of the $ClCO + Cl_2CO$, $CO + CCl_3O$, and $CO_2 + CCl_3$ channels.

(2) Vibrational Energy Disposal. Overall, the energy diagram of the $C_2Cl_3 + O_2$ reaction paths in Figure 6 shows deep wells in entrance and shallow barriers in exit, which suggests that the reaction intermediates are very short-lived. This explains well the experimental observation that the vibrational energies partitioned into CO is much more than that predicted by

statistical model. Similar nonstatistical dynamics behavior has been observed in many highly exothermic radical reactions.[21]

4. Conclusions

In summary, step-scan TR-FTIR emission spectroscopy has been used to characterize thoroughly the products, channels, vibrational energy disposal, and mechanism of the multichannel free radical reaction of C_2Cl_3 with O_2. Vibrationally excited products of Cl_2CO, CO, and CO_2 are observed in the IR emission spectra. Three major reaction channels forming respectively $ClCO + Cl_2CO$, $CO + CCl_3O$, and $CO_2 + CCl_3$ are therefore identified. The vibrational state distribution of the product CO is derived by fitting the IR emission spectra, and it is found that CO is highly vibrationally excited with the nascent average vibrational energy determined to be 59.9 kJ/mol. The surprisal analysis shows that the experimentally measured CO vibrational energy is much larger than that predicted by the statistical model, suggesting that the reaction proceeds through short-lived reaction intermediates. This nonstatistical dynamics behavior is consistent with the G3MP2 calculated energetics of the overall reaction paths, which shows deep wells in entrance and shallow barriers in exit. The $C_2Cl_3 + O_2$ reaction is a barrierless addition–elimination mechanism by first forming a peroxy intermediate C_2Cl_3OO* and then rearranging to a crucial three-member-ring COO intermediate through which the oxygen atoms are inserted into the C=C double bond of CCl_2=CCl radical, leading eventually to small products of Cl_2CO, CO, and CO_2.

References and Notes

(1) Laufer, A. H.; Fahr, A. *Chem. Rev.* **2004**, *104*, 2813 and references therein.

(2) Wang, H.; Wang, B.; He, Y.; Kong, F. *J. Chem. Phys.* **2001**, *115*, 1742.

(3) Russell, J. J.; Seetual, J. A.; Gutman, D.; Senkan, S. M. *J. Phys. Chem.* **1989**, *93*, 1934.

(4) Wang, H.; Li, J.; Song, X.; Li, Y.; Hou, H.; Wang, B.; Su, H.; Kong, F. *J. Phys. Chem. A* **2006**, *110*, 10336.

(5) Seakins, P. W. *The Chemical Dynamics and Kinetics of Small Radicals*; Liu, K., Wagner, A., Eds.; World Scientific: Singapore, 1995; pp 250−314.

(6) Osborn, D. L. *J. Phys. Chem. A.* **2003**, *107*, 3728.

(7) Chen, S. H.; Chu, L. K.; Chen, Y. J.; Chen, I. C.; Lee, Y. P. *Chem. Phys. Lett.* **2001**, *333*, 365.

(8) Wu, C. Y.; Lee, Y. P.; Ogilvie, J. F.; Wang, N. S. *J. Phys. Chem. A* **2003**, *107*, 2389.

(9) Lim, K. P.; Michael, J. V. *J. Phys. Chem.* **1994**, *98*, 211.

(10) Green, B. D.; Caledonia, G. E.; Murphy, R. E.; Robert, F. X. *J. Chem. Phys.* **1982**, *76*, 2441.

(11) Su, H.; Yang, J.; Ding, Y.; Feng, W.; Kong, F. *Chem. Phys. Lett.* **2000**, *326*, 73.

(12) Wang, B. S.; Gu, Y. S.; Kong, F. *J. Phys. Chem. A.*, **1998**, *102*, 9367.

(13) Stephenson, J. C.; Mosburg, E. R., Jr. *J. Chem. Phys.* **1974**, *60*, 3562.

(14) James, A. D.; Eunsook, S. H.; Karen, J. C.; Gary, D. D. *J. Phys. Chem. A* **2004**, *108*, 10965.

(15) Hewitt, A. D.; Brahan, K. M.; Boone, G. D.; Hewitt, S. A. *Int. J. Chem. Kinet.* **1996**, *28*, 763.

(16) Imamura, T.; Chono, H.; Shibuya, K.; Washida, N. *Int. J. Chem. Kinet.* **2003**, *35*, 310.

(17) Upadhyaya, H. P.; Kumar, A.; Naik, P. D.; Sapre, A. V. *Chem. Phys. Lett.* **2000**, *321*, 411.

(18) Muckerman, J. T. *J. Phys. Chem.* **1989**, *93*, 179.

(19) Hall, G. E.; Metzler, H. W.; Muckerman, J. T.; Preses, J. M.; Weston, R. E., Jr. *J. Chem. Phys.* **1995**, *102*, 6660.

(20) Levine, R. D.; Bernstein, R. B. *Molecular reaction dynamics and chemical reactivity*; Oxford University Press: Oxford, U.K., 1987.

(21) Donaldson, D. J.; Okada, Z. V.; Sloan, J. J. *J. Chem. Phys.* **1995**, *193*, 37.